Hybrid ceramic nanofiltration membranes prepared by impregnation and solid-state grafting of organo-phosphonic acids

Nikos Kyriakou, Elmar Boorsma, Gert-Jan Aardema, Guido Ritsema van Eck, Martin Drobek, Sissi de Beer, Arian Nijmeijer, Louis Winnubst, Marie-Alix Pizzoccaro-Zilamy

Journal of Membrane Science 687 (2023) 122041

Contents lists available at ScienceDirect

Journal of Membrane Science

journal homepage: www.elsevier.com/locate/memsci

Hybrid ceramic nanofiltration membranes prepared by impregnation and solid-state grafting of organo-phosphonic acids

Nikos Kyriakou [a], Elmar Boorsma [a], Gert-Jan Aardema [a], Guido Ritsema van Eck [b], Martin Drobek [c], Sissi de Beer [b], Arian Nijmeijer [a], Louis Winnubst [a], Marie-Alix Pizzoccaro-Zilamy [a,*]

[a] Inorganic Membranes, MESA+ Institute for Nanotechnology, University of Twente, 7500 AE, Enschede, the Netherlands
[b] Sustainable Polymer Chemistry, Department of Molecules & Materials, MESA+ Institute for Nanotechnology, University of Twente, 7500 AE, Enschede, the Netherlands
[c] Institut Européen des Membranes, Univ Montpellier, CNRS-UM-ENSCM, Place Eugène Bataillon, 34095, Montpellier, Cedex 5, France

ARTICLE INFO

Keywords:
Gamma alumina
Grafting
Phosphonic acid
PEG oligomers
Polymer brush
Nanofiltration
Hybrid ceramic membranes

ABSTRACT

Grafting of oligomers into the mesopores of ceramic membranes (e.g. γ-alumina) represents an attractive strategy for deploying durable, resistant, and efficient hybrid membranes for the industrial treatment of wastewater containing organic solvents and divers solutes. In general, to control the membrane/solute/solvent interactions, homogeneous surface modification and high grafting yields are required. However, reaching this goal is rather challenging with the current grafting approaches where the active diffusion of the oligomers to the membrane pore surface may be hampered. To mitigate such diffusion limitation, we present here a novel synthesis method consisting of an infiltration of concentrated PEG organophosphonic acid oligomer solution in ceramic ultrafiltration membranes before initiating the solid-state grafting reaction to form a PEG-brush-grafted nanofiltration ceramic membrane. The infiltration step was found to be decisive for the formation of weak bonds between the oligomer linking functions and the ceramic membrane ensuring the final synthesis of robust PEG-based membranes by a grafting reaction. The influence of the solvent polarity (water vs. cyclohexane) on the conformation of the grafted PEG brush inside the γ-alumina mesopores was observed as a key parameter in the analysis of the pore size and permeability results. In addition to this, it was studied here for the first time by molecular dynamic simulations. The as-prepared PEG-brush/ceramic membranes were found very efficient in the separation of small organic dyes such as Rhodamine B (479 g mol^{-1}) up to 85%. As a result, the present synthesis method represents a sustainable and simple alternative way for the preparation of hybrid nanofiltration membranes with controlled surface properties and attractive separation performance. Moreover, the vacuum impregnation and solid-state grafting approach requires a minimal amount of functional oligomers and solvent (0.5 mmol for 2–3 mL of solvent) and can be applied to other porous materials used in separation technologies.

1. Introduction

Ceramic nanofiltration membranes are often used for solvents or wastewater treatment applications [1–3]. However, most of these membranes do not possess the required durability or long-term performance when exposed to a mixture of solvents and solutes [4,5]. One of the main reasons for such undesirable behaviour bears on the formation of either weak or strong bonds between the solvent or solute molecules and the ceramic membrane surface rich in hydroxyl groups. Indeed, it must be underlined that this phenomenon often leads to a decrease in membrane performance over time [6]. Numerous attempts have therefore already been undertaken to improve and adapt the surface chemistry of such membrane materials to obtain solvent-resistant ceramic nanofiltration (NF) membranes.

Surface modification approaches are one of the most promising strategies for improving the performance of solvent-resistant nanofiltration ceramic membranes [3,7,8]. In particular, the covalent attachment of oligomers has been explored to form separation barriers driven by chemical affinities, possibly accompanied by molecular sieving separation mechanisms [9–11]. In this hybrid or grafted ceramic membrane [3], the defined and rigid pore structure of the ceramic membrane acts as the backbone that ensures the confinement of the

* Corresponding author.
E-mail address: m.d.pizzoccaro@utwente.nl (M.-A. Pizzoccaro-Zilamy).

https://doi.org/10.1016/j.memsci.2023.122041
Received 3 August 2023; Received in revised form 28 August 2023; Accepted 31 August 2023
Available online 2 September 2023

grafted molecules or oligomers. It is therefore the combination of the ceramic porous structure and the properties of the grafted oligomers that will drive the membrane separation properties. Polydimethylsiloxane (PDMS) oligomers (n = 10) bearing alkoxysilane leaking group were for example grafted on mesoporous γ-alumina membranes, resulting in higher rejections of Sudan Black B (>80%) from isopropanol, ethyl acetate, and toluene in comparison to the pristine ceramic membranes (<14%) [12]. In another paper [13], pre-synthetized polyethylene-glycol (PEG) alkoxysilane oligomers with various functional groups and different ethylene glycol units were used to functionalize low ultrafiltration-range γ-alumina membranes for solvent-resistant nanofiltration. The membranes showed an improved molecular weight-cut off compared to the pristine membrane when tested for the removal of Sudan Black B from ethanol and hexane (retention increased from ≈20 to 89 and 54%). However, as shown in our recent work [14], using PEG-alkoxysilane can easily lead to a progressive decrease in membrane performance in an aqueous environment due to the limited stability of the alkoxysilane linking functional in water. In the same work, an alternative approach consisting of the chemical grafting of PEG-phosphonic acids oligomers was used to guarantee a stable water flux over time but, on the other hand, leads to a lower retention rate compared to PEG-alkoxysilane grafted membranes due to the limited grafting density. In Ref. [14], the membranes were prepared by the solution-phase method consisting of the immersion of the ceramic membrane into a diluted solution of the oligomers followed by reflux. Under these reaction conditions, grafting is driven by the self-diffusion of the functionalized oligomers which limits the grafting density due to the steric hindrance or diffusion hampering caused by the very first grafted PEG brushes (Fig. 1, route a). To increase the grafting density, one can consider more concentrated solutions of oligomers and/or an application of harsher grafting conditions (temperature, pressure, harmful solvents etc.) [15,16]. Spray coating or support immersion followed by a thermal treatment in solid-state are possible alternatives recently described in the literature to prepare uniform hydrophobic monolayers of alkyl-based phosphonic acid molecules covalently bonded to metal oxide surfaces [17]. However, this grafting approach has never been used to modify pores with a diameter inferior to 10 nm. In general, the control of the grafting density of the polymer brushes can be obtained by surface-initiated polymerization method, but its implementation tends to be laborious [18]. Hence, a more straightforward method using a minimum amount of solvent without reflux or pressure-controlled systems for the preparation of PEG-brush grafted ceramic membranes would be a real asset in the area of solvent-resistant nanofiltration.

With this in mind, we propose here a novel approach to prepare PEG-functionalized nanofiltration ceramic membranes via the vacuum impregnation of a concentrated PEG-phosphonic acid oligomer solutions followed by a thermal treatment in the solid-state to overcome diffusion limitation during the pore surface functionalization (Fig. 1, route b). The vacuum impregnation method has been already employed elsewhere to prepare thin polymeric films or functionalized membranes prior to solution phase grafting [19,20]. However, this approach has never been used for the impregnation of phosphonic-based oligomers. It should be underlined that the vacuum impregnation combined with the grafting in the solid-state features two principal advantages: *i) application of low solvent quantities, and ii) absence of any reflux or a pressure-controlled system*. Two PEG organophosphonic acid oligomers, bearing an end group of different nature (i.e., hydroxyl vs methyl for PEGPA and MPEGPA, respectively; see Fig. 1) were selected to study the influence of the end group on the resulting grafting performance. The possibility to use the impregnation/solid-state grafting method was first studied on mesoporous γ-alumina nanoplate-like powders to inspect the chemical environment of the grafted species and the grafting density as a function of the applied grafting temperatures. The successful grafting was confirmed through a series of analytical techniques including Fourier-transform infrared spectroscopy (FTIR), ^{27}Al and ^{31}P solid-state nuclear magnetic resonance (NMR), and thermogravimetric analysis (TGA). Next, the influence of the tortuosity of the membrane support on the diffusion of the studied organophosphorus oligomers was explored within the mesopores γ-alumina membrane (pore diameter 3.7 nm) supported on α-alumina macroporous supports. The resulting hybrid membranes with grafted PEG phosphonic acid brushes were characterized by cyclohexane permporometry, FTIR, EDS and aqueous dye retention tests. The results obtained were compared with PEG-hybrid membranes prepared by the solution-phase grafting approach. Molecular dynamic (MD) simulations were conducted to study the interactions between PEG polymer brush and both water or cyclohexane to support the discussion on their influence on the "effective" pore diameter and the resulting water permeance.

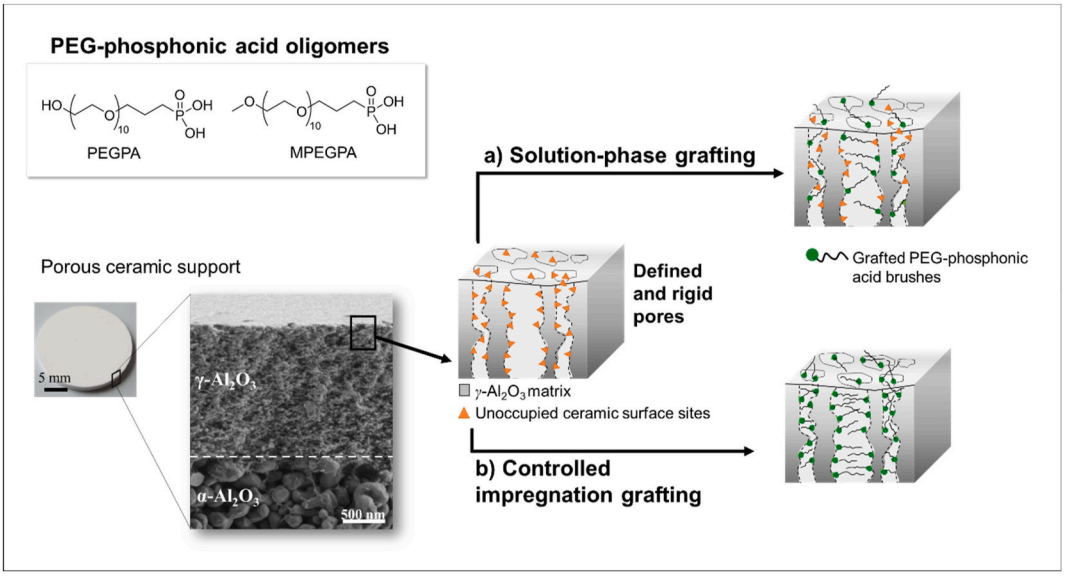

Fig. 1. Chemical structures of the phosphonic acid oligomers (PEGPA and MPEGPA) used in this work, with their corresponding abbreviations. The second part is a schematic illustration of the resulting hybrid membranes with grafted PEG phosphonic acid brushes prepared by (a) the solution-phase grafting and (b) the vacuum impregnation/solid-state grafting approach in a tortuous well-defined and rigid mesoporous γ-alumina matrix.

2. Materials and methods

2.1. Materials

Solvents methanol (analytical, 99%, Merck), ethanol (technical, Boom B·V.) and acetone (technical, Boom B·V.) were used as received. Polyethylene glycol ω-phosphonic acid (PEGPA, MW = 10, 580 g mol^{-1}) and Poly(ethylene oxide), α-methoxy, ω-phosphonic acid (MPEGPA, Mw = 10, 590 g mol^{-1}) were prepared according to the procedure used in our previous work [14] and thoroughly reported in Supplementary Information (SI) of this manuscript. The chemical structure of PEGPA and MPEGPA oligomers is provided in Fig. 1. Rhodamine B (RB, 99%, Merck) and Brilliant Yellow (BY, 70%, Sigma Aldrich) were used as received. Milli-Q water (18.2 MΩ cm) was applied in all synthesis and filtration experiments.

α-Alumina (α-Al_2O_3 > 99%) flat-sheet supports (discs with diameter 21 mm, thickness 2 mm, and 80 nm pore diameter) with one side polished were purchased from Pervatech B·V., the Netherlands. The polished side was dip-coated with a boehmite sol (prepared in-house) and subsequently calcined at 650 °C for 3 h. The dip-coating procedure was performed twice to avoid any potential defects in the resulting γ-alumina layer featuring 3.7 nm mean pore diameter and a total thickness of 3 μm (Polyethylene MWCO of 2500 Da) [21]. Further details concerning the fabrication and characteristics of the γ-alumina layers can be found elsewhere [22]. The as-prepared supports were washed with a water/ethanol solution (2:1 v/v) for at least 8 h, at room temperature, and finally dried and stored in a vacuum oven at 50 °C. For the equivalent γ-alumina nanopowder, the same boehmite sol and calcination procedure was used as previously. The resulting powder material was grinded into flake-like white nanopowder and stored in a dry atmosphere.

2.2. Vacuum impregnation and solid-state grafting of PEG-phosphonic acids oligomers on γ-alumina nanopowder

744 mg (1.3 mmol, 430 mM) PEGPA or 570 mg (0.9 mmol, 300 mM) of MPEGPA were dissolved in 2–3 mL of methanol at room temperature. Then, 1 g of γ-alumina nanopowders was added to the organophosphorus solution and the mixture was stirred vigorously for ~ 1 h at room temperature under gradually increasing vacuum until the methanol was removed. The impregnated nanopowders were then heated overnight to 60 °C (heating/cooling: 5 °C/min) under a nitrogen atmosphere to remove any remaining methanol from their porous structure. Impregnated γ-alumina nanopowders, with PEGPA or MPEGPA were called ImFP or ImFM, respectively. The subsequent grafting reaction was performed by thermal treatment of the impregnated samples at 150 °C or 200 °C for 12 h under nitrogen atmosphere (heating/cooling 5 °C/min). Then, the grafted nanopowders were washed with water followed by ethanol in a sonicated bath for 0.5 h and centrifuged between each washing step at 6000 rpm for 15 min. The washing procedure was repeated 3 times with each solvent. Grafted γ-alumina nanopowder samples were given a systematic name, where GFP or GFM represents the organophosphorus molecules used, respectively PEGPA, or MPEGPA while 150 or 200 relates to the temperature used for the thermal treatment.

2.3. Vacuum impregnation and solid-state grafting of PEG-phosphonic acids oligomers on γ-alumina membrane

290 mg (0.5 mmol) of PEGPA or 297.7 mg (0.5 mmol) of MPEGPA were dissolved in 5 mL of methanol (100 mM) at room temperature. Washed and dried supports were placed in a custom-made impregnation setup with the γ-alumina layer facing upwards. The impregnation was carried out by transferring the PEGPA or MPEGPA solution on top of the support and by applying vacuum for 0.5 h at room temperature. Then, the remaining solution (~4 mL) was removed with a Pasteur pipette and the wet membrane was dried at room temperature for 1 h. A schematic representation is given in Fig. S1 (SI). Finally, the membranes were transferred to an oven where the impregnated supports were heated overnight to 60 °C (5 °C/min) under a nitrogen atmosphere to remove any remaining methanol from the membrane pores. The subsequent grafting reaction was carried out by thermal treatment of the impregnated membranes at 150 or 200 °C for 12 h under a nitrogen atmosphere (heating/cooling 5 °C/min). After the grafting reaction, the membranes were backwashed with water in a dead-end permeation setup with a transmembrane pressure (TMP) of 30 bar applied on the α-alumina side of the membrane support. The washing procedure was performed during 3–5 days until no polymer was observed in the permeate. The removal of the unreacted species was monitored by using a double beam UV–Vis spectrophotometer (Shimadzu, UV-1800) (λ_{max} = 200 nm) comparing pure solvent with the washing aliquots. Grafted γ-alumina membrane samples were given a systematic name, where GP or GM represents the organophosphorus molecules used, respectively PEGPA, or MPEGPA while 150 or 200 relates to the temperature used for the thermal treatment.

2.4. Solution-phase grafting of PEG-phosphonic acids oligomers on γ-alumina membranes

The procedure as described by Kyriakou et al. [14] was used to prepare PEGPA and MPEGPA-grafted membranes by the solution-phase (SP) approach. The resulting grafted samples were annotated SP-P and SP-M when prepared respectively with PEGPA and MPEGPA.

2.5. Characterizations

Fourier Transform Infrared spectroscopy (FTIR) measurements on both membrane and powder samples were done using a PerkinElmer UATR Spectrum Two. Wavenumbers between 4000 and 400 cm^{-1} were scanned in reflectance mode at a resolution of 4 cm^{-1} for a minimum of 16 scans. The weight % of phosphorus and aluminium in the samples was determined by EDS using a Zeiss SEM (EVO HD15) at 10 kV with Oxford instruments software. The change in pore diameter of the membrane samples as a function of the grafting procedure was determined by permporometry using cyclohexane as condensable vapor. The experimental procedure is described in detail elsewhere [23]. X-ray diffraction (XRD) analysis was performed on a Bruker D2 phaser at the wavelength of Cu Kα (λ = 1.5405 Å; X-ray power: 40 kV, 40 mA) in Bragg-Brentano scanning mode between the angles 5 and 40° (2θ) scanned with a step size of 0.05°. The NMR measurements have been carried out at Institut Charles Gerhardt in Montpellier (France). Solid-state NMR spectra were acquired on a 600 MHz Varian VNMRS600 spectrometer ("Wide-bore" magnet at 14.09 T), using a Varian T3 MAS (Magic Angle Spinning) probe with 3.2 mm ZrO_2 rotors. All NMR experiments were performed at a spinning frequency of 20 kHz, and under temperature regulation to ensure that the temperature inside the rotor is 20 °C. ^{27}Al solid-state nuclear magnetic resonance (ssNMR) analysis were acquired using the quantitative Single Pulse technique with ^{1}H decoupling, with a recycle delay of 1 s and a π/12 pulse of 1 μs (~15°). Aluminium nitrate was used as a secondary reference (peak at 0.0 ppm). The width of the spectral window was 250 kHz and the line broadening 50 or 100 Hz. ^{31}P NMR spectra were acquired using the Cross Polarization technique with ^{1}H decoupling, with a recycle delay of 5 s, a contact time of 1.5 ms and a π/2 pulse of 4 μs (90°). Dipotassium phosphate has been used as a secondary reference (signal at 4.2 ppm). The width of the spectral window was 250 kHz and the line broadening 150 Hz. Water contact angles were measured using the sessile drop method, with 2 μL drops of Milli-Q water. Thermogravimetric analysis (TGA) was conducted using STA 449 F3 Jupiter (Netzsch). Measurements were performed under 55 mL min^{-1} N_2 and 15 mL min^{-1} O_2 flow with a heating rate of 5 °C/min from 40 to 800 °C. Temperature calibrations were made using melting standards. Measurements were run

sample-temperature controlled. The sample masses were determined, using an internal balance, 30 min after inserting the sample.

2.6. Evaluation of the membrane performance

Water permeability and retention data were collected with a custom-made, dead-end filtration setup, connected via a pressure regulator valve to a nitrogen tank. Permeability (L m^{-2} h^{-1} bar^{-1}) was expressed as the flux (L h^{-1}) of fluid across a membrane per unit of driving force and per square meter of exposed membrane area (2.4 x 10^{-4} m^2). Flux data were collected by measuring the mass of the permeate at four-time intervals, while permeability was determined from the slope of a linear fit of the collected flux data at applied transmembrane pressures between 5 and 20 bar. All slopes were found to be linear unless otherwise noted. Membranes were considered as impermeable (0 L m^{-2} h^{-1} bar^{-1}) to water after being evaluated at $\Delta P = 31$ bar overnight with no water flux detected.

Retentions (R) of Brilliant Yellow (BY, Mw = 624.55 g mol^{-1}, 50 ppm) and Rhodamine B (RB, Mw = 479.02 g mol^{-1}, 50 ppm) were conducted at a transmembrane pressure of 10 bar and were calculated by the equation:

$$R = 1 - c_p/c_f \quad (1)$$

where c_p and c_f are the permeate and feed solute concentrations, respectively. Retention samples were obtained at recoveries between 35 and 50%. Starting volumes were between 250 and 300 mL. Solute concentrations of BY and RB were calculated from PerkinElmer λ12 UV–Vis spectrophotometer measurements at the characteristic wavelengths of 401.5 and 543 nm for BY and RB in water respectively.

Retentates obtained during the water filtration tests and dye retention measurements were randomly tested by UV–Vis spectrophotometry for the potential presence of PEG-oligomers. In all cases nothing was detected, confirming that virtually no leaching of PEG-oligomers takes place, proving their strong anchoring to the support. Moreover, membrane samples were washed after each filtration test with both ethanol and water using ultrasonic treatments without any loss of membrane performance.

2.7. Molecular dynamic simulation setup

Molecular dynamic simulations of grafted PEG layers in cyclohexane and water were performed in LAMMPS (Large-scale Atomic/Molecular Massively Parallel Simulator) [24], using forcefield parameters and simulation settings derived from the coarse-grained Martini v2.0 forcefield [25]. Our simulation box measures 9.8 x 9.8 × 6 nm in x, y, and z directions respectively, and is periodic in x and y. The box is bounded by 9–3 Lennard-Jones potentials at 0 and 5.9 nm in z, modelling perfectly flat grafting surfaces that interact weakly with all species in the system. PEG is represented using a parametrization by Grunewald et al. [26], which specifically aims to capture energies of transfer between solvents of different polarity. Chains consist of 10 ether-oxide beads as defined in Ref. [26] capped by a standard Martini SP2 (small, weakly polar) bead at both ends, representing the terminal hydroxyl and the phosphonic acid anchoring group. Polymer brushes are built up on both sides of the simulation box by placing these PEG chains on a simple cubic 2D lattice at an areal density of 2.04 chains/nm^2, with one of the terminal SP2 beads at z = 0 for the lower brush, or at z = 5.9 nm for the upper brush. The SP2 beads at the grafting surfaces are excluded from time integration, effectively freezing them in place and thus mimicking anchoring of the chain. Simulations are run with the LAMMPS nve integrator, and thermostatted to a temperature of 298 K using a canonical-sampling velocity rescaling thermostat with a time constant of 300 fs [27]. After pre-equilibrating the PEG brushes, solvent particles are inserted into the simulation box, and the system is further equilibrated. While simulating in the canonical (NVT) ensemble allows for pressure fluctuations, here the system with solvent is in a nearly incompressible liquid state. These pressure fluctuations should therefore correspond to only minute fluctuations in density and composition, which do not qualitatively change the swelling behaviour of the PEG brush.

For the simulations in water, the solvent consists of 1737 P4 (strongly polar) Martini beads and 193 BP4 (strongly polar "antifreeze") beads, totalling 1930 solvent particles. It should be noted that by Martini conventions, each of these particles is assumed to represent a cluster of 4 water molecules. The 10% fraction of BP4 beads interacts identically to a P4 bead with other species but has different interaction parameters for the BP4–P4 interaction. This prevents the water from freezing while minimally altering its solvation behaviour. For simulations in cyclohexane, the solvent consists of 1300 cyclohexane molecules, which are represented as 3-membered rings of SC2 (small, slightly apolar) particles. These amounts of solvent particles were selected to produce similar equilibrium pressures in both systems. The masses of PEG and water particles were set to the Martini standard values of 45 and 72 g/mol respectively, as this closely matches the mass of the atoms they represent. The mass of the cyclohexane particles was set to 28 g/mol to match the molecular weight of cyclohexane at 84 g/mol for the full molecule.

To verify that the grafted chains form a brush, we performed simulations of a single free PEG chain in a 4 x 4 × 4 nm simulation box, filled with 740 water particles. This yielded a radius of gyration of approximately 7.2 Å for the free chain. Since the spacing between grafting points is set at 7 Å, the grafted PEG chains must experience significant excluded volume interaction, and we can assume the simulated PEG layers to display brush-like behaviour.

Density profiles (concentration as a function of z) for both solvent and PEG were saved every 200 ps over production runs of 200 ns. Comparing individual density profiles to the time-average over the full production run, we observed only random fluctuations, indicating that the system was in equilibrium during this period. A more extensive description of the simulation procedure is provided in the Supplementary Information, section 2.

3. Results and discussion

In this study, γ-alumina nanopowders and γ-alumina membranes were modified with either PEGPA or MPEGPA organophosphonic acid oligomers via impregnation/solid-state grafting. A concentrated oligomer solution was first infiltrated into the porous material structure under vacuum before conducting the solid-state grafting at elevated temperature and under an inert atmosphere. This method has been proven to be more attractive as compared to the conventional solution phase grafting method described in our previous work [14], especially in terms of the minimum amount of grafting solution used (less than 1 mL per cm^2) which favors the reuse of reagents and solvent. Since physically adsorbed PEG oligomers are removed during the washing procedure, only oligomers covalently bonded to the γ-alumina are assumed to remain on its surface.

3.1. Impact of temperature during vacuum impregnation and solid-state grafting

In the first place, the influence of temperature and/or the nature of the PEG oligomers' end group (i.e., methyl or hydroxyl) on the grafting yield was evaluated by thermogravimetric analysis (TGA) (Table 1, Figs. S4 and S5 and Table S4). Analysis of the impregnated γ-alumina nanopowder indicated a similar weight % of 34% (relative to the overall weight of γ-alumina plus PEG) for both PEGPA and MPEGPA. After the grafting reaction, the PEGPA-grafted samples showed a slight decrease in PEG weight % compared to the equivalent impregnated powders, typically 23 and 25% after reaction at 150 and 200 °C. This resulted in grafting yields (weight % PEG after impregnation/weight % PEG after grafting) of 68 and 74%, respectively. On the other hand, relatively low

Table 1
Calculated modification degree (expressed as grafting yield), based on TGA analysis on γ-alumina powders modified with different organophosphorus molecules (MPEGPA, and PEGPA) after impregnation and after a grafting reaction at 150 or 200 °C. Further details are given in SI-Figs. S4 and S5, and Table S4.

OrganoPA precursor	Weight % PEG after impregnation	Grafting reaction: 150 °C		Grafting reaction: 200 °C	
		Weight % PEG	Grafting yield (%)	Weight % PEG	Grafting yield (%)
PEGPA	34	23	68	25	74
MPEGPA	34	8	24	10	29

grafting yields of 24 and 29% were evidenced for MPEGPA samples prepared at 150 and 200 °C (Table 1). The high grafting yields of the PEGPA-grafted γ-alumina nanopowder might suggest a formation of crystalline or amorphous aluminium phosphonate phases due to dissolution–precipitation phenomena [28,29]. However, XRD (Fig. S6) and ^{27}Al solid-state NMR (Fig. S7) analysis for both PEGPA and MPEGPA samples did not detect any crystalline or amorphous aluminium phosphonate phases. When comparing the influence of the end group on the PEG chain, the highest grafting yield is obtained for PEGPA molecule containing the hydroxyl function.

FTIR analysis was used to confirm the grafting reaction of γ-alumina nanopowder with PEGPA and MPEGPA and evaluate any eventual differences in binding with the γ-alumina surface. The results are given in Fig. 2 and compared with the FTIR spectrum of the pristine γ-alumina which shows no significant absorption bands in the studied region. FTIR analysis of the pristine materials (PEGPA and MPEGPA) is characterized by the vibration bands of alkyl groups (C–H) between 1500 and 1250 cm^{-1} [30]. The strong vibrational band at 1090 cm^{-1}, accompanied by a small signal at 1034 cm^{-1}, is assigned to the asymmetric and symmetric vibration bands of the etheric repetitive unit. Furthermore, the bands appearing between 980 and 930 cm^{-1} for PEGPA and MPEGPA are attributed to the P–OH group in phosphonic acid [31]. Regarding the vibration bands attributed to the phosphoryl group (P═O) of the phosphonic acid functional group, the PEGPA exhibits no observable vibration band, while for MPEGPA the P═O vibration band is barely visible. This small, almost undetectable vibration band is attributed to the presence of the intermolecular interactions between the phosphonic acid and ether or hydroxyl functional groups of the brush chain resulting in broader, less intense, or invisible vibration bands [32].

After impregnation of the γ-alumina nanopowder with MPEGPA (ImFM), an FTIR spectrum relatively similar to the pure phosphonic acid molecule (MPEGPA) was recorded. In contrast, the impregnated samples prepared with PEGPA (ImFP) differ from the spectrum of the pure molecule in the region between 980 and 930 cm^{-1}, associated with the acid P–OH vibration bands. Here, the P–OH bond is only visible as a shoulder, while for the ImFM sample, the vibration bands associated with the P–OH bond are clearly observed. A possible explanation for the decrease in the vibration band intensity in the case of ImFP could be the presence of weak interactions between the phosphonic acid functions (P–OH, P═O) or the hydroxyl-end group (C–OH) of the PEG chain with the hydroxyl groups on the γ-alumina surface. This phenomenon may result in the establishment of a favourable binding configurations prior to grafting.

Following the thermal treatment and washing procedure, the grafting of PEGPA and MPEGPA was confirmed by the vanishing of the P–OH vibration bands in the FTIR spectra (GFP/GFM150) which indicates the formation of a covalent bond between the alumina surface and the phosphonic acid (P–O–Al) [30]. However, it must be noted that no new vibration bands related to the P–O–Al bond formation could be observed near the 1190 cm^{-1} IR region. A possible explanation for the lack of visibility of this P–O–Al vibration band could be the strong intensity of the C–O–C absorption band at 1090 cm^{-1}. As no P–OH bands are present after grafting, and the spectra were recorded after thoroughly washing the samples, it can be concluded (based on both TGA and FTIR results) that for all samples a covalent bond was formed between the PEG oligomers and the γ-alumina surface. Comparing the FTIR results from the different reaction temperatures, a more intense C–O–C band appears for the samples prepared at 200 °C compared to 150 °C. This can be related to additional material grafted on the inorganic surface with increasing temperature. Still, with solely FTIR, one cannot determine the influence of the temperature on the resulting binding modes formed between the phosphonic acid linking function and the inorganic surface under different temperatures.

To gain further insights into surface bonding, solid-state ^{31}P CP-MAS NMR spectroscopy analyses were conducted. Fig. 3 shows the ^{31}P CP-MAS NMR spectra of the impregnated and grafted PEGPA and MPEGA/γ-alumina nanopowder. Broad asymmetric signals originating from different chemical environments of the phosphorus atom can be

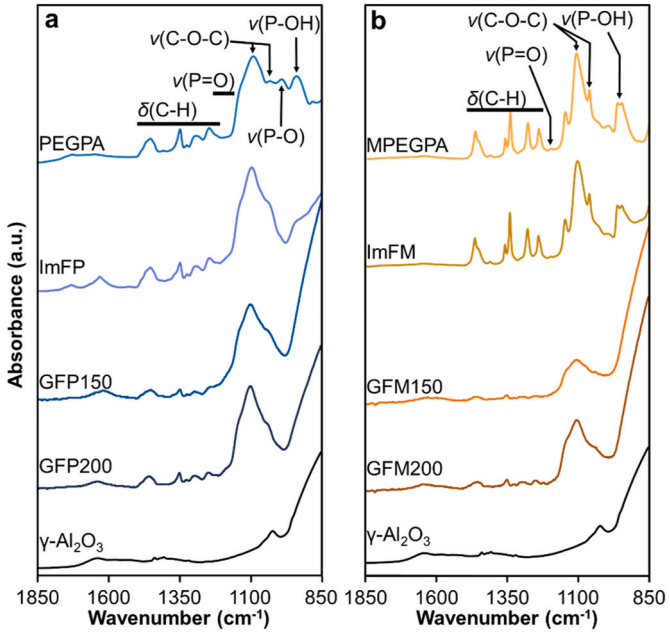

Fig. 2. FTIR spectra of PEGPA (a) and MPEGPA (b) in their pristine form, impregnated (ImF) on γ-alumina nanopowder and grafted on γ-alumina nanopowder at 150 °C (GFP/GFM150) and 200 °C (GFP/GFM200). The black line indicates the area where several C–H vibration bands can appear. For the P═O vibration band in the pure PEGPA oligomers, a range where it should appear according to the literature [33] is indicated by a black line.

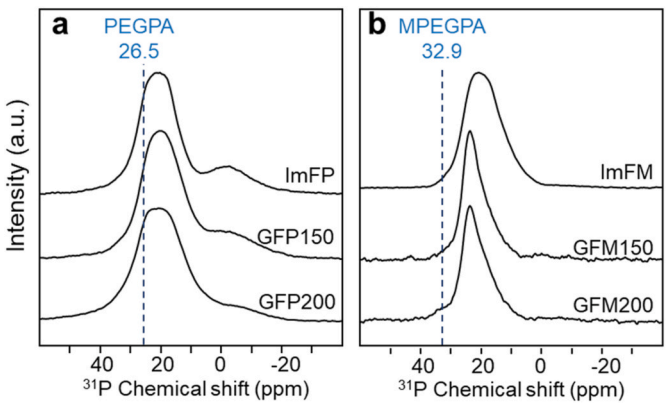

Fig. 3. ^{31}P CP-MAS NMR spectra of γ-alumina nanopowder impregnated (ImF) and grafted (GF) with PEGPA (a), and MPEGPA (b) at 150 and 200 °C. The main position of the pure PEG-phosphonic acid precursors is indicated with a dotted line and corresponds to the liquid ^{31}P NMR chemical shift reported in $CDCl_3$.

associated with different binding modes and surface conformations. The PEGPA-impregnated sample (ImFP) and the PEGPA-grafted samples (GFP150/200) present similar ^{31}P CP-MAS NMR spectra (Fig. 3). They are characterized by a main broad resonance centred at around 21.0 ppm which is shifted upfield with respect to the precursor resonance signal at 26.5 ppm in DMSO (Fig. S9). The similarity between the ^{31}P CP-MAS NMR spectra of the impregnated and grafted PEGPA samples suggests that the local environment of the phosphorus atom is similar before and after grafting. This finding supports the FTIR observations which suggested the setting of favourable binding modes prior to the grafting via the presence of weak interactions between the phosphonic acid function and the hydroxyl groups on the γ-alumina surface. The broad resonance observed at around 21.0 ppm is composed of at least two underlying signals at 18 and 24 ppm (Fig. S8). Moreover, an additional up field shoulder which could be attributed to phosphate-based compounds is visible between 0 and -15 ppm. After thermal treatment, its centre gradually shifts from −3 to −6 ppm and decreases in intensity with increasing grafting temperature. A possible explanation for the presence of this shoulder is the grafting of phosphate-based impurities, present in the bulk PEGPA such as monoester or diester, formed as a result of the McKenna reaction [34,35]. Another possibility is the presence of a side or self-condensation reaction that can occur between the hydroxyl-end group and the phosphonic acid linking group of PEGPA. The higher grafting density of PEGPA over MPEGPA was most likely caused by the more important self-condensation reaction of the former. As shown in Fig. S10, the PEGPA in its pristine form is a brown viscous liquid, however, after the thermal treatment at 200 °C, it transforms into a solid film (PEG200). On the other hand, the thermal treatment of MPEGPA (MPEG200) does not significantly change its visual aspect. FTIR analyses of both PEGPA and MPEGPA oligomers before and after the thermal treatment are presented in Fig. S11. No spectroscopic differences were observed for the MPEGPA samples treated at 150 or 200 °C in comparison to the pure oligomer. Contrary, unlike pure oligomer (PEGPA), the PEGPA150 and 200 samples showed a different intensity ratio for the doublet band attributed to the asymmetric and symmetric vibration of P–OH groups at 988 cm $^{-1}$. Besides, the esterification of acid functional groups was deduced by the presence of a new vibration band at 1035 cm^{-1} thus supporting the assumption of a self-condensation reaction.

Similar to PEGPA, upon impregnation, a broad envelope is visible between 34 and 10 ppm for the PEGPA grafted samples, but with a sharper main resonance signal after grafting centred at 24 ppm and an upfield shoulder centred around 18 ppm. The pure MPEGPA precursor has a sharp resonance signal at 32.9 ppm in $CDCl_3$ [14]. The sharper signal observed for the grafted samples could indicate a relatively lower diversity in surface conformations after grafting as compared to PEGPA.

From the FTIR and ^{31}P CP-MAS NMR results, it can be concluded that the binding modes of PEGPA and MPEGPA with the γ-alumina surface differ. In both cases, the PA linking group can interact with the etheric backbone and the inorganic surface via hydrogen bonds (green dotted line, Fig. 4a and b). In contrast, PEGPA chains can interfere intermolecularly with other PEGPA molecules via self-condensation reactions leading to a higher grafting yield as evidenced by TGA (Fig. 4a).

3.2. Membrane characteristics

Here, methanol was also selected as a solvent to prepare concentrated PEG-phosphonic acids oligomer solutions with low viscosity and to ensure fast solvent evaporation after the impregnation step. The γ-alumina membranes used in this work were 3 μm thick, featuring a defined and rigid porous structure with a pore diameter of 3.7 nm and a porosity of ~60%. Such membranes were used to study the effect of the grafting temperature upon the nanoconfinement of PEG-phosphonic acids in the γ-alumina porous structure and to determine the best conditions for controlling the pore functionalization and the membrane separation performance. Regarding the membrane preparation conditions, various concentrations of PEG-phosphonic acid oligomer solutions were tested before determining the optimum concentration (100 mM) to ensure a sufficient shrinkage of the γ-alumina pores. The impregnation via pressure was found to lead to inhomogeneity in the sample preparation and was therefore replaced by a vacuum. The surface properties of the grafted membranes were studied with water contact angle analysis (results are provided in Table S7) and compared with the results obtained for γ-alumina membranes made through solution-phase grafting of PEG-phosphonic acids [12]. Overall, the results confirm that regardless of the grafting method, the PEG-grafted membranes show a hydrophilic character (induced by the etheric units), which is significantly less than for the pristine inorganic surfaces containing hydroxyl groups.

FTIR analysis was performed on the grafted membranes and the results are provided in Fig. 5. In general, all spectra of the grafted samples (GP/GM150 and GP/GM200) exhibit absorption bands similar to those obtained for the grafted γ-alumina nanopowder (Fig. 2) and solution-phase grafted membranes [14]. Similarly, for the grafted γ-alumina

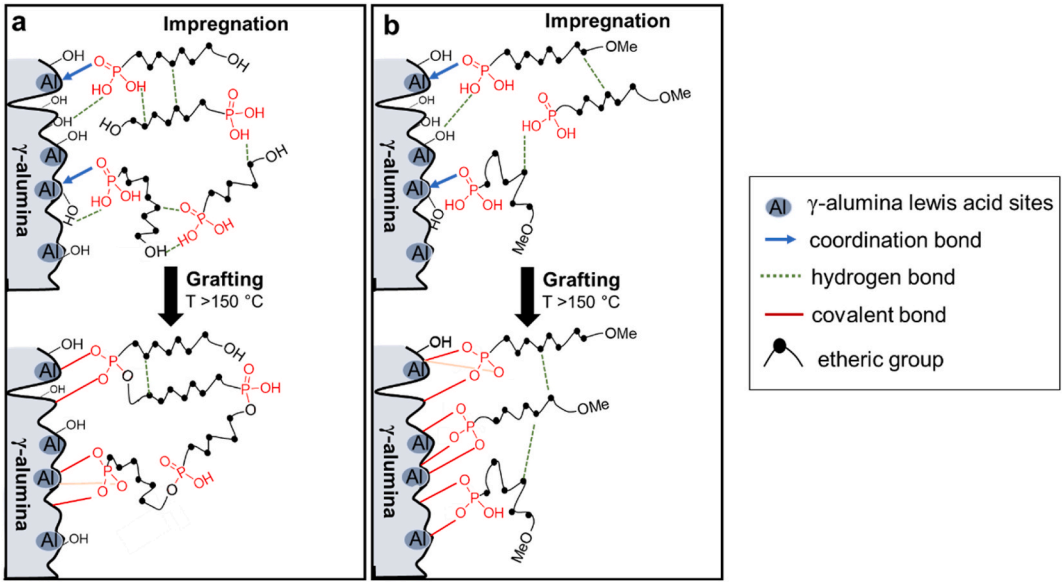

Fig. 4. Schematic representation of the impregnation and grafting of PEGPA (a) and MPEGPA (b).

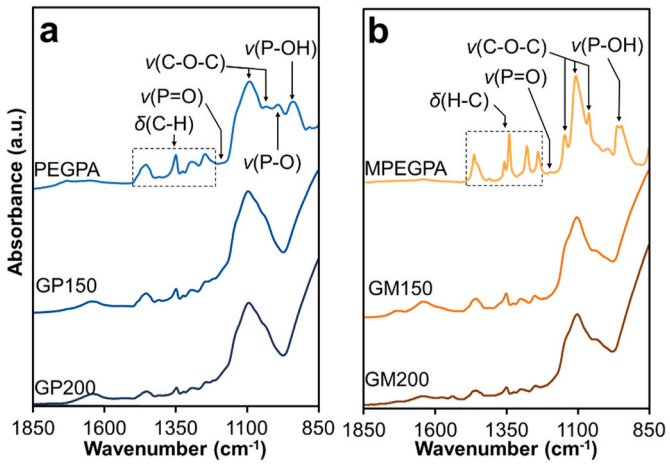

Fig. 5. FTIR spectra of the γ-alumina layer (γ-Al_2O_3), pure and grafted with PEGPA (a) and MPEGPA (b) at 150 (GP/GM150) and 200 °C (GP/GM200).

nanopowder, the P–O–Al bond overlaps with the C–O–C absorption band and is therefore not visible with FTIR. To make sure that the observed bands belong only to grafted PEGs, the membranes were thoroughly washed till no MPEGPA or PEGPA molecules could be detected in the permeate via UV analysis.

The distribution of the PEGPA polymer in the γ-alumina membranes grafted at different temperatures was analysed by SEM-EDS to estimate the P/Al ratio across the γ-alumina layer. The SEM-EDS results of the PEGPA grafted samples and the corresponding SEM micrographs are provided in Fig. S13. Overall, the GP150 and GP200 membranes exhibit a similar distribution of phosphorus over the γ-alumina membrane layer. The phosphorus distribution is uniform up to the penetration depths of 1.5 μm in the γ-alumina membrane layer and shows a decrease in concentration between 1.5 and 3 μm from the membrane surface. Grafting of oligomers in the α-alumina support was not detected by EDS as it can occur only scarcely due to the limited number of available hydroxyl surface groups. This illustrates that the impregnation step is, indeed, forcing the diffusion of the oligomers in the membrane pores. Even though TGA analysis on grafted powder showed an increase in the grafting yield with increasing reaction temperature, SEM-EDS analysis on the membranes indicates a similar distribution of PEG, independent of the temperature. This can be related to the measurement limitation of SEM-EDS providing only a rough estimation of the material amount in the samples. Furthermore, the EDS technique cannot be used to distinguish values related to the membrane top surface from the pore due to beam-induced artefacts resulting from the high voltage (10 kV) and spot size (50 nm in diameter). Therefore estimating the thickness of the separation layer using this technique is not possible. XPS analysis was not considered to answer this question due to the rough and porous nature of the ceramic support, which will also lead to less accurate results compared to flat and dense support. Hence, a pore size distribution analysis measured by cyclohexane permporometry was used as an indirect tool to characterize the grafting yield and thus assess the impact of the grafting method on the pore surface functionalization.

Cyclohexane permporometry was employed to shed more light on the influence of the grafting conditions on the final pore size of the prepared hybrid membranes. Prior to the analysis, the applicability of the Knudsen equation during cyclohexane capillary condensation was confirmed by conducting single gas permeation tests on the grafted membrane samples (Table S7). The results of the oxygen permeance as a function of the cyclohexane partial pressure during the desorption mode are presented in Fig. S14 for both the pristine γ-alumina membrane and PEG-grafted membranes prepared by impregnation followed by solid-state grafting.

From these permporometry data, pore size distributions were calculated, and the results are given in Fig. 6. In addition to the results of the pristine and PEGPA/MPEGPA grafted γ-alumina membranes prepared by the impregnation/solid-state grafting method, this figure also displays the results of PEGPA/MPEGPA membranes prepared by solution-phase grafting [14]. The pristine inorganic support shows a relatively narrow pore diameter distribution with a mean Kelvin radius of 2.3 nm. Solution-phase grafted samples are characterized by a narrow pore size distribution centred at a Kelvin radius of 1.9 and 2.1 nm respectively for PEGPA and MPEGPA. PEGPA impregnation-grafted sample prepared at 150 °C (GP150) resulted in a less steep transition in the oxygen permeance during the desorption of the cyclohexane vapours (Fig. S14) which was translated into a broadening of the pore size distribution values with two mean Kelvin radius centred at 1.1 and 1.7 nm. On the other hand, MPEGPA-impregnation grafted samples show a steeper transition, with a narrow pore size distribution centred at a Kelvin radius of 1.8 nm. The broadening in pore size distribution for the GP150 samples is probably caused by the self-condensation reaction. Overall, the samples prepared by impregnation-/solid-state grafting show a smaller pore radius compared to its solution-phase grafted analogues, thus suggesting an increased nanoconfinement through grafting PEGPA/MPEGPA brushes [14]. This result indirectly confirms the assumption that the impregnation/solid-state grafting allows increasing the grafting density in the pores. Samples treated at 200 °C with PEGPA (GP200) and MPEGPA (GM200) exhibited constant oxygen permeance at low relative cyclohexane pressures without any observed permeation increase (Fig. S14). This observation implies that the pore diameters are outside the range of applicability of the Kelvin equation (below 2 nm). Hence, the cyclohexane permporometry results suggest that a higher pore shrinkage can be achieved during solid-state grafting at 200 °C. A possible explanation could be based on a higher grafting density as observed for the grafted γ-alumina powders (Table 1). Considering that the grafting temperature increase can enhance the mobility of the polymeric chains in the γ-alumina pore, the PEG chains can stretch more by their extension from mushroom to brush-like morphology. As a result, additional PEGPA or MPEGPA brushes can be grafted next to each other on the pore surface. Surprisingly, the SEM-EDS results indicated a similar distribution of the PEGPA brushes over the γ-alumina membrane for the samples prepared at 150 and 200 °C. Such similar distribution of PEGPA brushes, but differences in pore radius could be explained by an increase of self-condensation reactions resulting in the formation of a tight cross-linked network at 200 °C and thus leading to higher pore shrinkage at higher grafting temperatures.

The influence of the grafting strategy (solution-phase vs. impregnation/solid-state grafting) on membrane' permeability was further studied through water flux measurements at 3 different transmembrane pressures, resulting in water permeabilities values as reported in Fig. 7. The membranes prepared by impregnation/solid-state grafting at 150 °C (GP150/GM150) present slightly lower, but almost identical water permeabilities (0.5–0.7 L m^{-2} h^{-1}. bar^{-1}) as reported previously for solution-phase PEG-grafted samples (0.6–0.7 L m^{-2} h^{-1}. bar^{-1}) [14]. By increasing the impregnation-grafting temperature to 200 °C, the PEGPA-grafted membranes (GP200/GM200) showed a strong decrease in water permeability (≤0.1 L m^{-2} h^{-1}. bar^{-1}). These lower water permeabilities are most likely related to the higher grafting density and/or formation of a cross-linked network as evidenced by permporometry.

Regarding the tenfold decrease in water permeability of PEG grafted membranes (SP–P/M, GP/GM150) compared to pristine γ-alumina membranes, Tanardi et al. [13] showed (by conducting permeation tests in solvents of various polarities) that higher flow resistance to water is possibly due to solvent sorption on the grafted PEG brushes. To confirm this assumption, in this work, molecular dynamic (MD) simulations were conducted to study the interaction between grafted PEG oligomers and water or cyclohexane molecules in slit-shaped pores as present in γ-alumina membranes.

Fig. 8 shows a snapshot of the simulation box after the insertion of

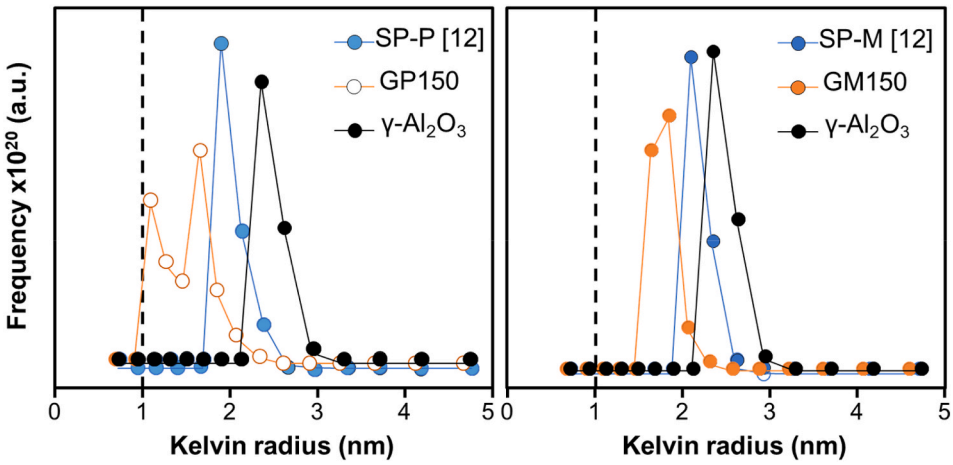

Fig. 6. Calculated Kelvin pore radius distributions from cyclohexane permporometry for the pristine and PEGPA and MPEGPA grafted membranes prepared by impregnation/solid-state grafting and solution-phase grafting [14]. The dark dotted line at a Kelvin radius of 1 nm represents the applicability limit of the Kelvin equation.

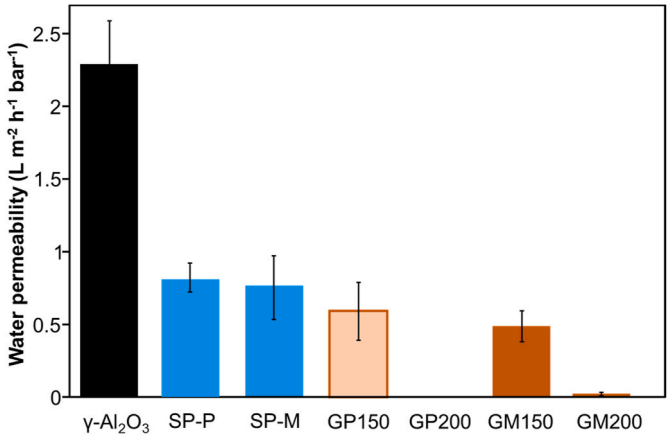

Fig. 7. Water permeability of pristine γ-alumina membranes, and PEGPA/MPEGPA grafted γ-alumina membranes prepared by solution-phase (SP–P, SP-M) and impregnation/solid-state grafting (GP/GM150 and 200). Error bars indicate the standard deviation between three membranes prepared under similar conditions.

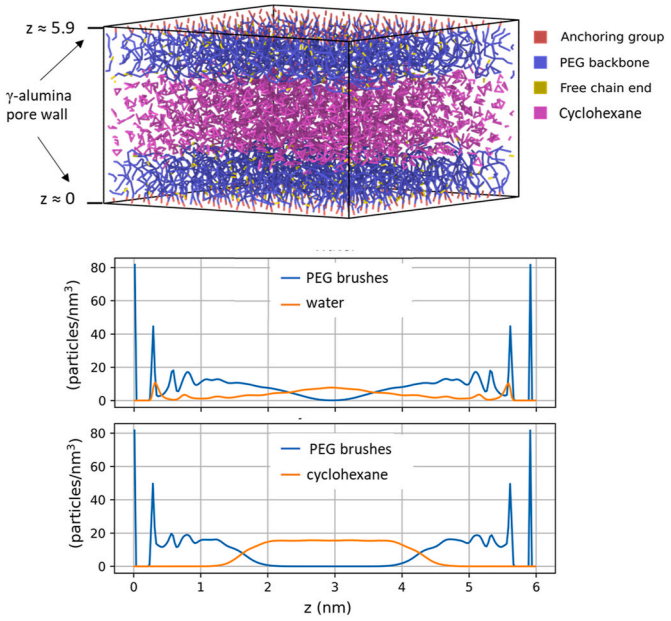

Fig. 8. Snapshot of the simulation box after insertion of cyclohexane molecules and the resulting number density as a function of z for PEG and water or cyclohexane recovered from molecular dynamics simulations. Time-averaged over the final 200 ns of the simulation.

cyclohexane molecules. The γ-alumina pore is represented in three dimensions assuming a slit shape with a pore width of 5.9 nm. The grafting surfaces are located at fixed positions representing the pore wall on the z-axis (z ≈ 0 and 5.9 nm). The resulting density profiles for PEG and solvent molecules (water or cyclohexane) over the z-direction of the simulation box are shown in Fig. 8. In both density profiles, high, narrow peaks in PEG density can be seen at both grafting surfaces (at z ≈ 0 and 6 nm), since all chains are anchored at the same height. The secondary peaks further away from the grafting surfaces can similarly be attributed to the 10 ether oxide beads along each PEG chain, which have a well-defined equilibrium distance from the anchoring site because of bond and angle interactions. While a slight density oscillation can be seen due to similar minima further along the chain, meaning the PEG concentration decays more or less continuously away from the surface for the remainder of the profile. This parabolically shaped decay is typical for grafted polymers in good media (like water in the case of PEG polymer), and reflects the entropic loss incurred by the chains upon stretching [36].

When solvated by water, the PEG chains are highly extended, with the two brushes almost overlapping [36] in the middle of the system. The solvent distribution indicates that water penetrates the entire PEG layer. Slight enrichments in solvent can be seen at the outer edge of the mathematical wall (at the second peak in the PEG profiles), indicating adsorption of water particles at the grafting surface. In the cyclohexane-solvated system, on the other hand, the PEG brushes are more collapsed, and the cyclohexane is concentrated in the centre of the simulation box. The cyclohexane concentration rapidly falls to zero deeper in the brushes, indicating that little to no absorption occurs in the grafted layer.

These findings support that the polarity of the solvent contributes strongly to the swelling of the PEG brush. It is possible that this polarity-based solvent preference is enhanced by volume effects. The simulated PEG brushes have a grafting density of 2.04 chain/nm^2 and hence a spacing of 0.7 nm between chains, before accounting for the volume of the PEG chains themselves. The Martini representation of cyclohexane measures roughly 0.73 nm along its largest dimension, whereas water particles (cluster of 4 water molecules) have an approximate diameter of 0.47 nm. It therefore seems plausible that cyclohexane entering the

brush would experience steric hindrance, while this is less likely for the water particles.

In conclusion, the MD simulation results support the assumption that the high resistance of water flux observed in the MPEGPA/PEGPA grafted membranes is caused by a possible swelling due to water sorption in the grafted moieties. It should be noted that in real industrial wastewater treatment, one should consider not only the presence of water but also the presence of apolar organic solvents possibly limiting the swelling phenomena and thus increasing the final membrane permeability.

3.3. Dye retention tests

Finally, retention tests were performed with Brilliant Yellow (BY, 629 Da) and Rhodamine B (RB, 479 Da) on PEGPA and MPEGPA hybrid membranes prepared via the solution-phase (SP–P) and impregnation/solid-state grafting approach (GP150, GM150 and GM200). The membranes were repeatedly ultrasonically washed after each filtration test and it has been confirmed that no PEG oligomers were detected in the washing solvent thus confirming the stability of the membrane materials. The results are given in Fig. 9. All grafted membranes showed BY retention. On the other hand, the RB retentions varied between the different samples studied. The membranes SP-P, GM150, and GM200 exhibited RB retentions superior to 70%, while the GP150 membrane showed no difference in retention compared with the pristine support (~15%) [37]. Interestingly, GM150 membranes featured significantly higher RB retention than GP150 samples, while GP150 shows a smaller pore diameter than GM150 when analysed by cyclohexane permporometry (Fig. 6). This observation could be attributed to the effect of the self-condensation reactions of PEGPA occurring in the GP150 membrane and thus leading differences in the solvent/PEG-network interactions. One could also clearly observe the differences in RB retention between samples prepared by the solution phase and impregnation/solid-state grafting of PEGPA. Reaching such a high dye retention for the solution phase sample can furthermore be induced by the adsorption of RB via carboxylate bonds on free sites of the γ-alumina pore surface (a lower grafting yield observed). Therefore, it is reasonable to assume that the RB dye adsorbed in the SP-P samples also contributes to the >70% RB retention performance as dipole-dipole interactions between charged RB molecules and γ-alumina can increase the overall membrane separation performance.

The performance comparison of the membranes prepared in this work by solution-phase (SP–P) and impregnation/solid-state grafting (GM150) with other relevant hybrid ceramic/inorganic membrane materials reported in the literature is shown in Fig. 10. To allow a comparison with a wider range of hybrid ceramic membranes, performance results reported using isopropanol and ethanolic dye solutions were used assuming that the charge of dye molecules is similar in polar solvents [38]. It must be emphasized that a direct comparison with surface-functionalized polymeric membranes is not realistic due to the swelling behaviour and wide pore size distribution of conventional polymeric membranes. Hence, only hybrid membranes prepared on porous ceramic supports are included in Fig. 10. The water permeability of the used pristine γ-alumina membrane (not primarily designed for water filtration applications) is relatively low (respectively 7.7 and 5.9 $L\,m^{-2}\,bar^{-1}\,h^{-1}$ for α and α+γ alumina supports). It is however expected that improvement of membrane permeability can be achieved by reducing the thickness of the mesoporous intermediate layer and by increasing the pore size and porosity of the α-alumina macroporous part of the support. As evidenced in Fig. 10, GM150 features a high potential interest for the applications in the NF range because of the excellent dye retention of 84% for RB (459 Da), and 94% for BY (624 Da). As expected, the dye retentions of the PEG-grafted membrane have increased substantially compared to pristine ultrafiltration γ-alumina membrane support with RB and BY retention of 14% and 76%, respectively [39]. Both dye molecules are electrostatically charged in water media, however, it is assumed that the increased retention observed for BY results mainly from a dominant size-exclusion separation mechanism as recently reported for PSf-b-PEG membranes [40]. It must be noted that higher retentions were reported for cross-linked organic networks made of polyimide and polyphosphazene with similar alumina supports. Such results could be possibly attributed to the more narrow pore size distribution in comparison with the PEG-grafted membranes [37,39].

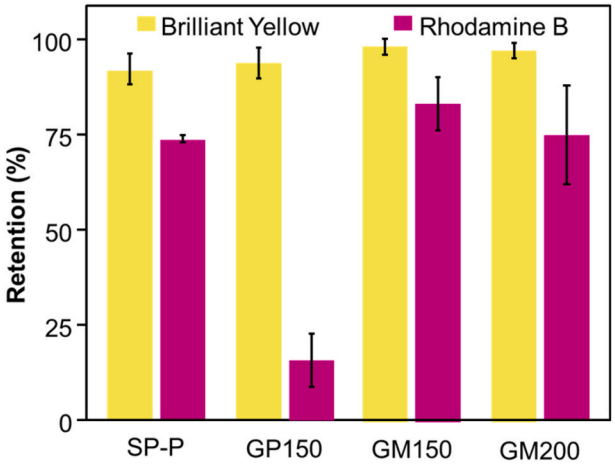

Fig. 9. Dye (in water) retention of the PEGPA/MPEGPA grafted γ-alumina membranes prepared by solution-phase and impregnation/solid-state grafting. 50 ppm of Brilliant Yellow (624 Da) or Rhodamine B (479 Da) in water were used for the nanofiltration tests. (For interpretation of the references to colour in this figure legend, the reader is referred to the Web version of this article.)

4. Conclusion

In this work, we have shown for the first time the preparation of PEG-grafted mesoporous γ-alumina membranes ($Ø_{pore} \approx 3.7$ nm) for nanofiltration application via a vacuum impregnation of concentrated PEG oligomer solutions followed by a solid-state grafting. FTIR and ^{31}P solid-

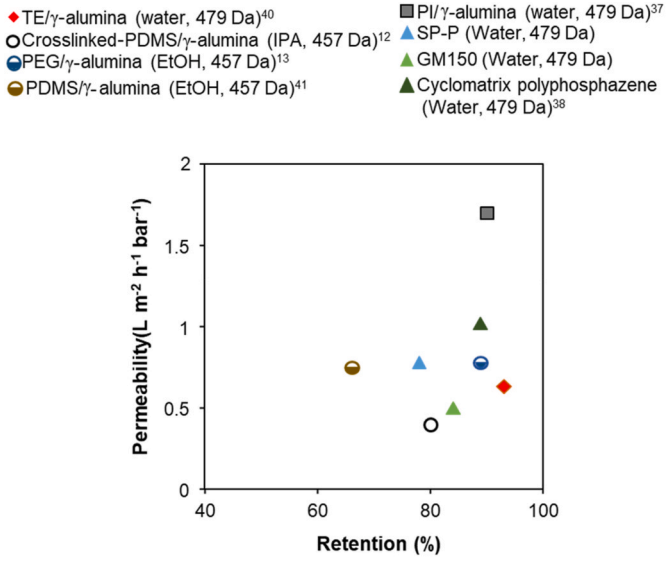

Fig. 10. Comparison of the best-performing membrane from this work prepared by solution-phase (SP–P) and impregnation/solid-state grafting (GM150) with other membranes reported in the literature (solvents and Mw of dyes studied are given in brackets and listed in Table S8) [12,13,37,39,41,42]. The membranes used in this figure are similar in terms of the support or the membrane layer used (γ-alumina).

state NMR analysis has confirmed the formation of covalent bonds between the PEG-phosphonic acid oligomers and the γ-alumina surface. TGA results indicated an important influence of the hydroxyl end group in the PEG-phosphonic acid (PEGPA) oligomer resulting in significantly higher grafting densities compared to the γ-alumina powders functionalized with methoxy-terminated PEG-phosphonic acid (MPEGPA). A secondary self-condensation reaction identified between PEGPA oligomers during grafting was confirmed to be avoided when employing a methoxy-terminated PEG-phosphonic acid (MPEGPA). Grafting of the PEG oligomers in membranes at 200 °C resulted in larger pore shrinkages ($Ø_{pore} \leq 2$ nm) compared to grafting performed at lower temperatures (150 °C) ($Ø_{pore} \approx 3$ nm). This finding indicates a synergistic effect between polymer nanoconfinement and reaction temperature on the grafting density on the pore surface. MPEGPA-grafted γ-alumina membranes exhibit a high RB (Mw of 459 g mol^{-1}) retention (84%) while maintaining acceptable water permeance. Low water permeability values from 0.5 to 0.7 L m^{-2} h^{-1}. bar^{-1} could be explained by the high hydraulic resistance of the applied alumina support and possible swelling of the PEG-grafted brushes as shown by MD simulations. Indeed, this work is among the first attempts to use MD simulations to evaluate the potential of functionalized ceramic membranes for solvent nanofiltration. It clearly demonstrates MD simulation potential to become a precious tool for predicting the separation performance of grafted membranes in the challenging field of solvent-resistant nanofiltration. Finally, it should be underlined that the impregnation/solid-state grafting method described in this work represents a straightforward strategy that can be potentially expanded to other organophosphonic acids (alkyl-chain of different length, polystyrene, polydimethylsiloxane, polymethyl methacrylates etc.), and inorganic supports (ZrO_2, TiO_2, SiO_2, SiC) to fabricate materials with varying surface and pore properties. Further research is currently in progress transferring the optimized synthesis protocol for an up-scaled synthesis on commercial porous tubular ceramic supports with an active surface area of up to 4.4 m^2. The obtained results will be the object of our next communication.

CRediT authorship contribution statement

Nikos Kyriakou: Initiated the work and performed most of the experiments, characterization and performance tests, and wrote the first draft. **Elmar Boorsma:** carried out grafting on powders and membranes, and the self-condensation reactions. **Gert-Jan Aardema:** conducted gas permeation and initial/exploratory MD simulation tests. **Guido Ritsema van Eck:** designed and conducted final MD simulations. **Martin Drobek:** supervised the NMR analysis, review & editing. **Sissi de Beer:** supervised the MD simulation work. **Arian Nijmeijer:** provided general input to this research especially on interpreting transport properties. **Louis Winnubst:** responsible for funding acquisition, joint daily supervisor of PhD student Nikos Kyriakou on this project; Gave detailed scientific input during the progress of this research, review & editing. **Marie-Alix Pizzoccaro-Zilamy:** joint daily supervisor of the PhD student Nikos Kyriakou on this project, weekly discussion with the PhD student on progress, gave detailed scientific input during the progress of this research, writing of the final draft, review & editing.

Authors statement

The authors confirm that no AI tools were used in the research and writing process of this manuscript.

Declaration of competing interest

The authors declare the following financial interests/personal relationships which may be considered as potential competing interests: Louis Winnubst reports financial support was provided by Institute for Sustainable Process Technology.

Data availability

No data was used for the research described in the article.

Acknowledgments

This work is part of the research program entitled 'Solvent Tolerant Nanofiltration and reverse osmosis membranes for the purification of industrial aqueous streams' (STNF) conducted within the framework of the Institute for Sustainable Process Technology (ISPT, project no BL-20-12). Emmanuel Fernandez (Assistant de Recherche CNRS) from the Institute Charles Gerhardt in Montpellier, France is sincerely acknowledged for his helpful contribution to NMR analysis. The authors also thank Frank Morssinkhof and Herman Teunis for their assistance in respectively liquid filtration testing and SEM analysis. Prof. Vera Meynen and Dr. Anita Buekenhoudt are also thanked for their input on the first version of this manuscript.

Appendix A. Supplementary data

Supplementary data to this article can be found online at https://doi.org/10.1016/j.memsci.2023.122041.

References

[1] T. Arumugham, N.J. Kaleekkal, S. Gopal, J. Nambikkattu, R.K.A.M. Aboulella, S. Ranil Wickramasinghe, F. Banat, Recent developments in porous ceramic membranes for wastewater treatment and desalination: a review, J. Environ. Manag. 293 (2021), https://doi.org/10.1016/j.jenvman.2021.112925.
[2] M.B. Asif, Z. Zhang, Ceramic membrane technology for water and wastewater treatment: a critical review of performance, full-scale applications, membrane fouling and prospects, Chem. Eng. J. 418 (2021), https://doi.org/10.1016/j.cej.2021.129481.
[3] R.B. Merlet, M.-A. Pizzoccaro-Zilamy, A. Nijmeijer, L. Winnubst, Hybrid ceramic membranes for organic solvent nanofiltration: state-of-the-art and challenges, J. Membr. Sci. 599 (2020), https://doi.org/10.1016/j.memsci.2020.117839.
[4] S. Rezaei Hosseinabadi, K. Wyns, V. Meynen, R. Carleer, P. Adriaensens, A. Buekenhoudt, B. van der Bruggen, Organic solvent nanofiltration with Grignard functionalised ceramic nanofiltration membranes, J. Membr. Sci. 454 (2014) 496–504, https://doi.org/10.1016/j.memsci.2013.12.032.
[5] T. van Gestel, B. van der Bruggen, A. Buekenhoudt, C. Dotremont, J. Luyten, C. Vandecasteele, G. Maes, Surface modification of g-Al2O3/TiO2 multilayer membranes for applications in non-polar organic solvents, J. Membr. Sci. 224 (2003) 3–10, https://doi.org/10.1016/S0376-7388(03)00132-7.
[6] G.G. Paradis, Novel Concepts for Microporous Hybrid Silica Membranes: Functionalization and Pore Size Tuning, 2012, https://doi.org/10.3990/1.9789036533669.
[7] V. Meynen, H. Castricum, A. Buekenhoudt, Class II hybrid organic-inorganic membranes creating new versatility in separations, Curr. Org. Chem. 18 (2014) 2334–2350, https://doi.org/10.2174/1385272819666140806200931.
[8] J.G. van Dijck, P. Mampuys, H.Y.V. Ching, D. Krishnan, K. Baert, T. Hauffman, J. Verbeeck, S. van Doorslaer, B.U.W. Maes, M. Dorbec, A. Buekenhoudt, V. Meynen, Synthesis – properties correlation and the unexpected role of the titania support on the Grignard surface modification, Appl. Surf. Sci. 527 (2020), https://doi.org/10.1016/j.apsusc.2020.146851.
[9] M.-A. Pizzoccaro-Zilamy, M. Drobek, E. Petit, C. Totée, G. Silly, G. Guerrero, M. G. Cowan, A. Ayral, A. Julbe, Initial steps toward the development of grafted ionic liquid membranes for the selective transport of CO2, Ind. Eng. Chem. Res. 57 (2018), https://doi.org/10.1021/acs.iecr.8b02466.
[10] J.J. Keating, J. Imbrogno, G. Belfort, Polymer brushes for membrane separations: a review, ACS Appl. Mater. Interfaces 8 (2016) 28383–28399, https://doi.org/10.1021/acsami.6b09068.
[11] L.A. Smook, G.C. Ritsema Van Eck, S. de Beer, Friends, foes, and favorites: relative interactions determine how polymer brushes absorb vapors of binary solvents, Macromolecules 53 (2020) 10898–10906, https://doi.org/10.1021/acs.macromol.0c02228.
[12] C.R. Tanardi, A. Nijmeijer, L. Winnubst, Coupled-PDMS grafted mesoporous γ-alumina membranes for solvent nanofiltration, Sep. Purif. Technol. 169 (2016) 223–229, https://doi.org/10.1016/j.seppur.2016.05.057.
[13] C.R. Tanardi, R. Catana, M. Barboiu, A. Ayral, I.F.J. Vankelecom, A. Nijmeijer, L. Winnubst, Polyethyleneglycol grafting of y-alumina membranes for solvent resistant nanofiltration, Microporous Mesoporous Mater. 229 (2016) 106–116, https://doi.org/10.1016/j.micromeso.2016.04.024.
[14] N. Kyriakou, M.A. Pizzoccaro-Zilamy, A. Nijmeijer, M. Luiten-Olieman, L. Winnubst, Hydrolytic stability of PEG-grafted γ-alumina membranes: alkoxysilane vs phosphonic acid linking groups, Microporous Mesoporous Mater. 307 (2020), https://doi.org/10.1016/j.micromeso.2020.110516.

[15] A. Roevens, J.G. Van Dijck, D. Geldof, F. Blockhuys, B. Prelot, J. Zajac, V. Meynen, Aqueous or solvent based surface modification: the influence of the combination solvent – organic functional group on the surface characteristics of titanium dioxide grafted with organophosphonic acids, Appl. Surf. Sci. 416 (2017) 716–724, https://doi.org/10.1016/j.apsusc.2017.04.143.
[16] M.A. Pizzoccaro-Zilamy, S.M. Piña, B. Rebiere, C. Daniel, D. Farrusseng, M. Drobek, G. Silly, A. Julbe, G. Guerrero, Controlled grafting of dialkylphosphonate-based ionic liquids on γ-alumina: design of hybrid materials with high potential for CO2 separation applications, RSC Adv. 9 (2019) 19882–19894, https://doi.org/10.1039/c9ra01265f.
[17] G.A.L. Andreatta, N. Blondiaux, J. Gay, S. Unterhofer, A. Lachowicz, A. Faes, Spray coating vs. immersion for self-assembly of gemini perfluorinated phosphonic acids on indium tin oxide, Thin Solid Films (2021) 732, https://doi.org/10.1016/j.tsf.2021.138783.
[18] R.B. Merlet, M. Amirilargani, L.C.P.M. de Smet, E.J.R. Sudhölter, A. Nijmeijer, L. Winnubst, Growing to shrink: nano-tunable polystyrene brushes inside 5 nm mesopores, J. Membr. Sci. 572 (2019) 632–640, https://doi.org/10.1016/j.memsci.2018.11.058.
[19] J.A. Howarter, J.P. Youngblood, Amphiphile grafted membranes for the separation of oil-in-water dispersions, J. Colloid Interface Sci. 329 (2009) 127–132, https://doi.org/10.1016/j.jcis.2008.09.068.
[20] M.J.T. Raaijmakers, W. Ogieglo, M. Wiese, M. Wessling, A. Nijmeijer, N.E. Benes, Sorption behavior of compressed CO2 and CH4 on ultrathin hybrid poly(POSS-imide) layers, ACS Appl. Mater. Interfaces 7 (2015) 26977–26988, https://doi.org/10.1021/acsami.5b08286.
[21] M.-A. Pizzoccaro-Zilamy, C. Huiskes, E.G. Keim, S.N. Sluijter, H. Van Veen, A. Nijmeijer, L. Winnubst, M.W.J. Luiten-Olieman, New generation of mesoporous silica membranes prepared by a stöber-solution pore-growth approach, ACS Appl. Mater. Interfaces 11 (2019), https://doi.org/10.1021/acsami.9b03526.
[22] R.J.R. Uhlhorn, M.H.B.J. Huis in't Veld, K. Keizer, A.J. Burggraaf, Synthesis of ceramic membranes Synthesis of non-supported and supported y-alumina, J. Mater. Sci. 27 (1992) 527–537.
[23] F.P. Cuperus, D. Bargeman, C.A. Smolders, Permporometry: the determination of the size distribution of active pores in UF membranes, J. Membr. Sci. 71 (1992) 57–67, https://doi.org/10.1016/0376-7388(92)85006-5.
[24] A.P. Thompson, H.M. Aktulga, R. Berger, D.S. Bolintineanu, W.M. Brown, P. S. Crozier, P.J. in 't Veld, A. Kohlmeyer, S.G. Moore, T.D. Nguyen, R. Shan, M. J. Stevens, J. Tranchida, C. Trott, S.J. Plimpton, Lammps - a flexible simulation tool for particle-based materials modeling at the atomic, meso, and continuum scales, Comput. Phys. Commun. 271 (2022), https://doi.org/10.1016/j.cpc.2021.108171.
[25] S.J. Marrink, H.J. Risselada, S. Yefimov, D.P. Tieleman, A.H. de Vries, The MARTINI force field: coarse grained model for biomolecular simulations, J. Phys. Chem. B 111 (2007) 7812–7824, https://doi.org/10.1021/jp071097f.
[26] F. Grunewald, G. Rossi, A.H. de Vries, S.J. Marrink, L. Monticelli, Transferable MARTINI model of poly(ethylene oxide), J. Phys. Chem. B 122 (2018) 7436–7449, https://doi.org/10.1021/acs.jpcb.8b04760.
[27] G. Bussi, D. Donadio, M. Parrinello, Canonical sampling through velocity rescaling, J. Chem. Phys. 126 (2007), https://doi.org/10.1063/1.2408420.
[28] M.A. Pizzoccaro-Zilamy, S.M. Piña, B. Rebiere, C. Daniel, D. Farrusseng, M. Drobek, G. Silly, A. Julbe, G. Guerrero, Controlled grafting of dialkylphosphonate-based ionic liquids on γ-alumina: design of hybrid materials with high potential for CO2 separation applications, RSC Adv. 9 (2019), https://doi.org/10.1039/c9ra01265f.
[29] G. Guerrero, P.H. Mutin, A. Vioux, Organically modified aluminas by grafting and sol–gel processes involving phosphonate derivatives, J. Mater. Chem. 11 (2001) 3161–3165, https://doi.org/10.1039/b104411g.
[30] R. Luschtinetz, G. Seifert, E. Jaehne, H.J.P. Adler, Infrared Spectra of Alkylphosphonic Acid Bound to Aluminium Surfaces, Macromol Symp, 2007, pp. 248–253, https://doi.org/10.1002/masy.200750837.
[31] A. Vega, P. Thissen, Y.J. Chabal, Environment-controlled tethering by aggregation and growth of phosphonic acid monolayers on silicon oxide, Langmuir 28 (2012) 8046–8051, https://doi.org/10.1021/la300709n.
[32] D. Lin-Vien, N.B. Colthup, W.G. Fateley, J.G. Grasselli, Organophosphorus compounds, in: The Handbook of Infrared and Raman Characteristic Frequencies of Organic Molecules, Elsevier, 1991, pp. 263–276, https://doi.org/10.1016/b978-0-08-057116-4.50022-5.
[33] M. Badertscher, P. Bühlmann, E. Pretsch, Structure Determination of Organic Compounds: Tables of Spectral Data, Springer Berlin, Heidelberg, 2009, https://doi.org/10.1007/978-3-540-93810-1.
[34] K. Justyna, J. Małolepsza, D. Kusy, W. Maniukiewicz, K.M. Błażewska, The McKenna reaction – avoiding side reactions in phosphonate deprotection, Beilstein J. Org. Chem. 16 (2020) 1436–1446, https://doi.org/10.3762/bjoc.16.119.
[35] M. Kim, M. Kobayashi, H. Kato, M. Kakihana, A highly luminous LiCaPO4:Eu2+; phosphor synthesized by a solution method employing a water-soluble phosphate ester, Opt Photon. J. 3 (2013) 13–18, https://doi.org/10.4236/opj.2013.36a003.
[36] S.T. Milner, T.A. Witten, M.E. Cates, A parabolic density profile for grafted polymers, Europhys. Lett. 5 (1988) 413, https://doi.org/10.1209/0295-5075/5/5/006.
[37] N. Kyriakou, L. Winnubst, M. Drobek, S. de Beer, A. Nijmeijer, M.-A. Pizzoccaro-Zilamy, Controlled nanoconfinement of polyimide networks in mesoporous γ-alumina membranes for the molecular separation of organic dyes, ACS Appl. Nano Mater. (2021), https://doi.org/10.1021/acsanm.1c03322.
[38] P. Marchetti, L. Peeva, A. Livingston, The selectivity challenge in organic solvent nanofiltration: membrane and process solutions, Annu. Rev. Chem. Biomol. Eng. 8 (2017) 473–497, https://doi.org/10.1146/annurev-chembioeng-060816-101325.
[39] F. Radmanesh, G. Bargeman, N.E. Benes, Cyclomatrix polyphosphazene organic solvent nanofiltration membranes, J. Membr. Sci. 668 (2023), https://doi.org/10.1016/j.memsci.2022.121215.
[40] Y. Liu, J. Wang, Y. Wang, H. Zhu, X. Xu, T. Liu, Y. Hu, High-flux robust PSf-b-PEG nanofiltration membrane for the precise separation of dyes and salts, Chem. Eng. J. 405 (2021), https://doi.org/10.1016/j.cej.2020.127051.
[41] N. Kyriakou, R.B. Merlet, J.D. Willott, A. Nijmeijer, L. Winnubst, M.A. Pizzoccaro-Zilamy, New method toward a robust covalently attached cross-linked nanofiltration membrane, ACS Appl. Mater. Interfaces 12 (2020) 47948–47956, https://doi.org/10.1021/acsami.0c13339.
[42] R.B. Merlet, C.R. Tanardi, I.F.J. Vankelecom, A. Nijmeijer, L. Winnubst, Interpreting rejection in SRNF across grafted ceramic membranes through the Spiegler-Kedem model, J. Membr. Sci. 525 (2017) 359–367, https://doi.org/10.1016/j.memsci.2016.12.013.